

Chemical Rescue of Phosphoryl Transfer in a Cavity Mutant: A Cautionary Tale for Site-Directed Mutagenesis^{†,‡}

Suzanne J. Admiraal,[§] Philippe Meyer,^{||} Benoit Schneider,[⊥] Dominique Deville-Bonne,[⊥] Joël Janin,^{||} and Daniel Herschlag^{*,§}

Department of Biochemistry, Beckman Center B400, Stanford University, Stanford, California 94305-5307, Laboratoire d'Enzymologie et Biochimie Structurales, CNRS UPR 9063, 91198 Gif-sur-Yvette, France, and the Unité de Régulation Enzymatique des Activités Cellulaires, CNRS URA 1773, Institut Pasteur, 25 rue du Dr. Roux, 75724 Paris Cedex 15, France

Received October 24, 2000

ABSTRACT: We have explored the ability of a nucleoside diphosphate kinase (NDPK) mutant in which the nucleophilic histidine has been replaced by glycine (H122G) to transfer phosphate from ATP to alcohols of varying pK_a , size, shape, and polarity. This cavity mutant does indeed act as a primitive alcohol kinase. The rate of its phosphoryl transfer to alcohols varies considerably, with values spanning a $\Delta\Delta G^\ddagger$ range of 4 kcal/mol, whereas the alcohols have very similar intrinsic reactivities. Analysis of these results suggests that the ability to carry out phosphoryl transfer within the cavity is not a simple function of being small enough to enter the cavity, but rather is a complex function of steric, solvation, entropic, van der Waals packing, and electrostatic properties of the alcohol. In addition, large differences are observed between the reactivities of alcohols within the nucleophile cavity of H122G and the reactivities of the same alcohols within the nucleophile cavity of H122A, a mutant NDPK that differs from H122G by a single methyl group within the cavity. The crystal structures of the two cavity mutants are very similar to one another and to wild-type NDPK, providing no evidence for a structurally perturbed active site. The differences in reactivity between the two mutant proteins illustrate a fundamental limitation of energetic analysis from site-directed mutagenesis: although removal of a side chain is generally considered to be a conservative change, the energetic effects of any given mutation are inextricably linked to the molecular properties of the created cavity and the surrounding protein environment.

Previous studies of small molecule rescue of either the reactivity or stability of cavity mutants have provided insights into protein energetics. Mutagenesis of the lysine general base of aspartate aminotransferase to an alanine allowed Toney and Kirsch to investigate the ability of exogenous amines to restore catalytic activity to this cavity mutant (7). Matthews and co-workers demonstrated that a variety of small, mainly nonpolar ligands stabilize a cavity mutant of T4 lysozyme (8–10). In both studies, the authors obtained an energetic picture of the primarily hydrophobic cavities that were investigated by varying the small molecule that occupied those cavities. These earlier results suggested that a systematic study of rescue in a more complex cavity that is accessible to solvent and bordered by charged residues could provide information about the energetic features of protein crevices such as those often present at active sites.

We have explored the energetic features of such a protein cavity using H122G, a site-directed mutant of nucleoside diphosphate kinase (NDPK)¹ in which the nucleophilic histidine has been replaced by a glycine. Wild-type NDPK interconverts NTPs and NDPs by catalyzing successive phosphoryl transfers, first transferring a phosphoryl group from an NTP to histidine 122 to form a phosphorylated enzyme and an NDP, then catalyzing a second transfer between the phosphorylated enzyme and another NDP. Although the H122G enzyme lacks a covalent nucleophile, previous work has shown that it can be chemically rescued for reaction with ATP by exogenous Im, primary amines, and water, which act as nucleophiles to form ADP and a phosphorylated nucleophile (Figure 1) (11). These nucleophiles appear to enter the cavity created by the histidine mutation and attack ATP in the H122G active site. These earlier findings suggested that energetic features of the H122G cavity could be explored by systematic variation of the rescuing nucleophile.

[†] This work was supported by a grant from the Packard Foundation to D.H. and by a grant from the Agence Nationale de Recherche contre le SIDA (ANRS) to J.J. P.M. acknowledges financial support from Sidaction. S.J.A. was a Howard Hughes Medical Institute Predoctoral Fellow.

[‡] Atomic coordinates for *Dictyostelium* H122A nucleoside diphosphate kinase have been deposited at the Protein Data Bank under the file name 1HLW.

* To whom correspondence should be addressed. Phone: (650) 723-9442. Fax: (650) 723-6783. E-mail: herschla@cmgm.stanford.edu.

[§] Stanford University.

^{||} Laboratoire d'Enzymologie et Biochimie Structurales.

[⊥] Institut Pasteur.

¹ Abbreviations: NDPK, *Dictyostelium* nucleoside diphosphate kinase; H122G, NDPK with His 122 replaced by Gly; H122A, NDPK with His 122 replaced by Ala; Im, imidazole; P_i, phosphate; ImP, imidazole phosphate; k_{rel} , rate constant relative to analogous water reaction; Tris-HCl, tris(hydroxymethyl)aminomethane hydrochloride; EPPS, 4-(2-hydroxyethyl)-1-piperazinepropanesulfonic acid; EDTA, ethylenediaminetetraacetic acid; PAGE, polyacrylamide gel electrophoresis; HPLC, high-performance liquid chromatography.

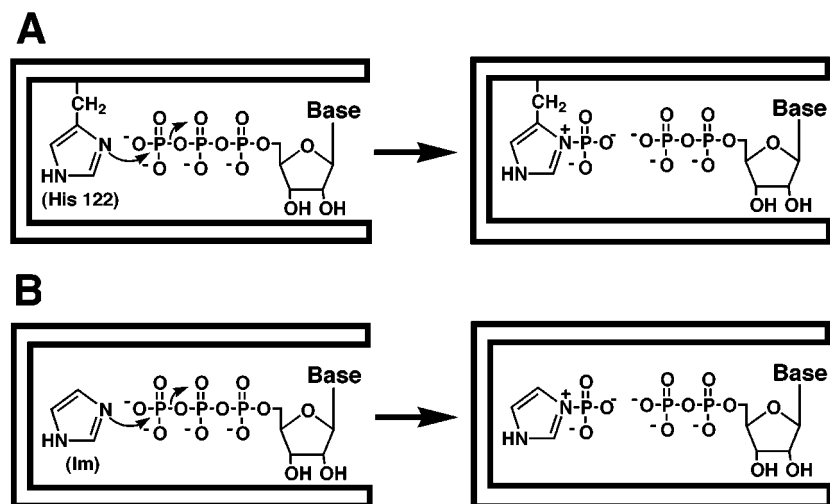


FIGURE 1: Reactions catalyzed by wild-type (A) and H122G (B) NDPK. The enzymes are represented by a thick outline. (A) Wild-type NDPK catalyzes the interconversion of NTPs via a histidyl phosphate covalent intermediate. The first step of this process, reaction of His 122 and an NTP to form the covalent intermediate and an NDP, is shown. The second step of the wild-type reaction is simply the reverse of this reaction with a different NDP. (B) Nucleophiles such as Im, shown here, can access the cavity created by the replacement of His with Gly in the H122G mutant and react with an NTP to form a phosphorylated nucleophile and an NDP.

Rescue of activity is a stringent probe of the surrounding protein context relative to rescue of stability because, after entering the cavity, the nucleophile must orient to react with the bound and positioned ATP molecule. By correlating the ability of nucleophiles to rescue phosphoryl transfer with physical characteristics of those nucleophiles, we sought to generate an energetic picture of the H122G cavity. Alcohol nucleophiles were selected to probe the mutant cavity because a large number of alcohols of varying pK_a , size, shape, and polarity are readily available. The study of alcohol reactivity was extended to include the H122A cavity mutant, and reactivity comparisons between alcohol and amine nucleophiles with identical R groups were performed for the H122G cavity mutant. Our results indicate that alterations in properties of both the nucleophile and the cavity have large and unexpected energetic consequences on rescue.

The complex energetic picture of the NDPK nucleophile cavity that emerges from this study highlights the inherent context dependence of energetic effects from site-directed mutagenesis.

EXPERIMENTAL PROCEDURES

Materials. Im was obtained from Baker, and alcohols were from Aldrich and were of the highest purity available. Ultrapure ATP was from Pharmacia; ADP and GDP were from Boehringer Mannheim. Unpurified $[\gamma\text{-}^{32}\text{P}]\text{ATP}$ was obtained from Amersham. Multiple radioactive bands were detected when radiolabeled ATP was analyzed by PAGE and exposed to film (Kodak), so it was purified by elution with water from 15% nondenaturing polyacrylamide gels prior to use in experiments. Water was doubly distilled from an all-glass apparatus.

Site-Directed Mutagenesis. H122G *Dictyostelium* NDPK was prepared by site-directed mutagenesis and characterized as described previously (11). H122A was prepared analogously, using the oligonucleotide 5'-GAAACATCATCGC-CGGTTCTGATTC-3'.

Enzyme Purification. Mutant *Dictyostelium* NDPKs were overexpressed in *Escherichia coli* (XL1-Blue) using plasmid *pndk* as described (12), with minor modifications. Both

proteins were purified as described previously for H122G and stored at $-20\text{ }^\circ\text{C}$ (11). Protein concentration was determined using the calculated extinction coefficient at 280 nm: $9200\text{ M}^{-1}\text{ cm}^{-1}$ (13). Enzyme concentration was expressed as concentration of 17 kDa subunits.

Reactions of H122 Mutants with Alcohols. Reactions of H122 mutants and ATP were performed at $25\text{ }^\circ\text{C}$ in the presence of a series of alcohol nucleophiles. Typical reactions contained $1\text{ }\mu\text{M}$ H122G or H122A, 2–15% alcohol, 50 mM potassium EPPS (pH 7.8), 5 mM MgCl_2 , and 100 nM ATP with trace $[\gamma\text{-}^{32}\text{P}]\text{ATP}$. In all reactions, ionic strength was maintained at 0.3 M (KCl). Reaction rates were linearly dependent upon ATP concentration under these conditions, indicating that ATP was subsaturating. The reactions were pH-independent between pH 7 and 9, suggesting that Glu 133, a residue in the proximity of the nucleophile cavity, was deprotonated under all conditions investigated. Reaction aliquots were removed at specified times and quenched by addition of an equal volume of 20 mM EDTA (pH 8). These aliquots were loaded onto an anion-exchange HPLC column (Dionex Nucleopac PA-100, $9 \times 250\text{ mm}$), and a LiCl gradient (0.01 to 1 M in 10% acetonitrile, 10 mM NaOH) was used to separate alkyl phosphate products from P_i and ATP. ^{32}P -Containing substrate and products were quantitated by scintillation counting. ATP and P_i peaks were identified by comparison to known standards. An additional radioactive peak that eluted prior to P_i and ATP appeared only in samples containing alcohol, and the amount formed was dependent on alcohol concentration; this peak was therefore identified as the alkyl phosphate product. Alkyl phosphate products were only detected in reactions that contained enzyme, and observed rates for water and alcohol reactions were dependent on enzyme concentration (the relative rate constants for reactions of alcohols with respect to reaction of water remained constant). The ratio of alkyl phosphate to P_i was constant throughout a particular time course, indicating that no secondary reactions involving the reaction products were occurring.

The relative rate constant (k_{rel}) for reaction of a given alcohol with respect to water was determined from the

Scheme 1

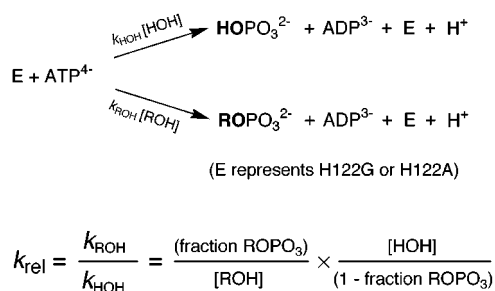


Table 1: Statistics on Crystallographic Analysis

diffraction data	
space group	<i>P</i> 6 ₃ 22
cell parameters (Å)	
a	75.00
b	75.00
c	106.17
resolution (Å)	1.9
measured intensities	110 350
unique reflections	13 910
completeness (%)	95.8
<i>R</i> _{merge} (%) ^a	6.9
refinement	
<i>R</i> _{cryst} (%) ^b	16.6 (20.8)
reflections	13 909
protein atoms	1142
solvent atoms	133
average <i>B</i> (Å ²)	28.6
geometry ^c	
bond distances (Å)	0.014
bond angle (deg)	1.9
torsion angle (deg)	1.16

^a $R_{\text{merge}} = \frac{\sum |I(h_i) - \langle I(h) \rangle|}{\sum I(h_i)}$. ^b $R_{\text{cryst}} = \frac{\sum ||F_o| - |F_c||}{\sum |F_o|}$ was calculated with CNS on all reflections. The value of *R*_{free} is in parentheses. ^c Root-mean-square deviation from ideal values.

alcohol concentration of the original reaction ([ROH]) and the fraction of total product present as alkyl phosphate, according to the equation in Scheme 1. For each alcohol, the same *k*_{rel} value, within error, was obtained for reactions performed at different alcohol concentrations. The rate constants for loss of ATP were within 5-fold in all cases, indicating that absolute reactivity was not greatly perturbed by the solvent changes. Each *k*_{rel} value in Table 2 represents an average of at least three separate HPLC runs; the average includes controls for different reaction pH, different reaction times, and different alcohol concentrations, as described above. Values of *k*_{rel} measured for individual alcohols varied over a range of <2-fold in different experiments.

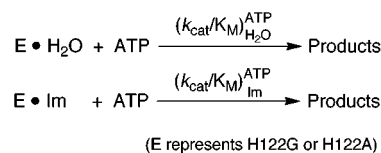
Reactions of H122 Mutants with Im or Water. Reactions were performed at 25 °C in buffered solutions of ionic strength 0.3 M (KCl) in the presence of 5 mM MgCl₂ and varying concentrations of Im and H122A or H122G (10–500 nM) to obtain (*k*_{cat}/*K*_M)^{ATP}_{Im} (Scheme 2). Analogous reactions were carried out without Im to follow the enzyme-catalyzed hydrolysis reaction [(*k*_{cat}/*K*_M)^{ATP}_{H₂O}; Scheme 2]. Reaction rates were linearly dependent on enzyme concentration. The reaction rates of the mutants with Im were pH independent between pH 7 and 9, so a buffer composition of 50 mM potassium EPPS, pH 7.8, was routinely used. Im stocks were adjusted to the reaction pH with small amounts of KOH. Reactions were initiated by the addition of substrate ATP (100–500 nM) containing trace [γ -³²P]ATP and aliquots were removed at specified times and quenched by

Table 2: Relative Rate Constants for H122G-Catalyzed Reactions of Alcohols and ATP⁴⁻·Mg²⁺^a

ROH	p <i>K</i> _a ^b	<i>k</i> _{rel}
HOH	15.7	(1)
(CH ₃) ₂ CHOH	17.1 ^c	0.0059 ± 0.0002
(CH ₃) ₂ CHCH ₂ OH	16.1 ^d	0.019 ± 0.012
CH ₃ CH ₂ CH(CH ₃)CH ₂ OH	16.1 ^d	0.090 ± 0.011
(CH ₃) ₂ CHCH ₂ CH ₂ OH	16.1 ^d	0.31 ± 0.02
CH ₃ CH ₂ CH ₂ OH	16.1 ^c	0.025 ± 0.002
CH ₃ CH ₂ CH ₂ CH ₂ OH	16.1 ^c	0.35 ± 0.04
CH ₃ CH ₂ CH ₂ CH ₂ CH ₂ OH	16.1 ^e	3.6 ± 0.2
CH ₃ CH ₂ CH ₂ CH ₂ CH ₂ CH ₂ OH	16.1 ^e	3.2 ± 0.4
CH ₃ CH ₂ OH	16.0	0.034 ± 0.006
H ₂ C=CHCH ₂ CH ₂ OH	15.9 ^f	0.16 ± 0.04
CClH ₂ CH ₂ CH ₂ OH	15.6 ^f	1.6 ± 0.3
H ₂ C=CHCH ₂ OH	15.5	0.51 ± 0.02
CH ₃ OH	15.5	0.18 ± 0.03
HC≡CCH ₂ CH ₂ OH	15.3 ^f	0.055 ± 0.009
HOCH ₂ CH ₂ OH	14.8	0.0064 ± 0.0014 ^g
CH ₃ OCH ₂ CH ₂ OH	14.8	0.084 ± 0.008
CH ₃ CH ₂ OCH ₂ CH ₂ OH	14.8 ^e	1.2 ± 0.1
CFH ₂ CH ₂ OH	14.3 ^h	0.0077 ± 0.0023
CClH ₂ CH ₂ OH	14.3	0.013 ± 0.006
N≡CCH ₂ CH ₂ OH	14.0	0.0033 ± 0.0019
HC≡CCH ₂ OH	13.6	0.20 ± 0.01
CH ₃ C≡CCH ₂ OH	13.6 ^e	0.83 ± 0.20
CF ₂ HCH ₂ OH	12.9 ^h	0.0049 ± 0.0033
CF ₃ CH ₂ OH	12.4	0.0010 ± 0.0002

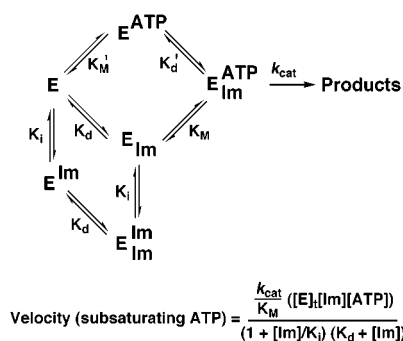
^a 25 °C, 50 mM potassium EPPS, pH 7.8, 5 mM MgCl₂, *I* = 0.3 M (KCl). ^b From ref 49 unless otherwise noted. ^c From ref 50. ^d Alcohols that are branched at C2 or C3 were assumed to have p*K*_a values identical to those of their unbranched counterparts; a branch at C1 increases the p*K*_a of 2-propanol by 1 unit relative to propanol, and branching further from the alcohol moiety is expected to have a much smaller effect. Different p*K*_a assignments for the branched alcohols would not affect any of the conclusions. ^e Pentanol and hexanol were assumed to have p*K*_a values identical to propanol and butanol, as the additional methylene groups several carbons removed from the alcohol moiety are not expected to perturb the p*K*_a. The same logic was used to assign the known p*K*_a of methoxyethanol to ethoxyethanol and to assign the known p*K*_a of propargyl alcohol to 2-butyne-1-ol. Different values of p*K*_a would not affect any of the conclusions. ^f 3-Buten-1-ol differs from allyl alcohol in that its substituent is located at C3 rather than at C2. Its p*K*_a was estimated by multiplying the p*K*_a difference between butanol (parent compound) and allyl alcohol by 0.3 and subtracting this value from the p*K*_a of butanol. The falloff factor of 0.3 for the movement of the substituent one methylene group further from the alcohol moiety was determined empirically from measured p*K*_a values of primary amines with identical C2 and C3 substituents (49). The p*K*_a values of chloropropanol and 3-buten-1-ol were estimated analogously using the p*K*_a values of propanol and chloroethanol or butanol and propargyl alcohol, respectively, as limits. Different values of p*K*_a would not affect any of the conclusions. ^g Statistically corrected for the presence of two alcohol groups. ^h Trifluoroethanol and trichloroethanol differ in p*K*_a by only 0.2 units (12.4 vs 12.2; 49). The p*K*_a values of fluoroethanol and difluoroethanol were therefore assumed to be the same as the p*K*_a values of chloroethanol and dichloroethanol, respectively. Different values of p*K*_a for fluoroethanol and difluoroethanol would not affect any of the conclusions.

Scheme 2



addition of an equal volume of 20 mM EDTA (pH 8) in 20% glycerol. Reaction rates were linearly dependent upon ATP concentration under these conditions, indicating that ATP was subsaturating. Radiolabeled substrate (ATP) and

Scheme 3



products (ImP and P_i) were separated by electrophoresis on 15% nondenaturing polyacrylamide gels, and their ratios at each time point were quantitated with a Molecular Dynamics PhosphorImager. Data analysis was performed using Kaleidagraph (Synergy Software), and exponential fits to the data typically gave $R \geq 0.99$.

Analysis of Im Binding and Saturation for H122A NDPK. A modest downward curvature was observed in the Im dependence of the H122A reaction with ATP at the highest Im concentrations (see Figure 7 below), as had been seen previously in the Im dependence of the H122G reaction with ATP (11). As in the earlier work, this curvature was presumed to arise from binding of an inhibitory Im to the nucleotide base site, in addition to the Im that binds and rescues in the nucleophile site. An inhibitory Im would be expected to bind similarly to the base sites of wild-type NDPK, H122G, and H122A, so a binding constant of 0.45 M was assigned to the inhibitory H122A site based on the Im inhibition of wild-type NDPK (11). The saturation data for H122A were then fit to a model with two Im, one that serves as the nucleophile and one, with a $K_i = 0.45$ M, that is responsible for the inhibition, as diagrammed in Scheme 3.² The data fit well to this model, with $K_d = 1.0$ M for binding of Im to the nucleophile site and $(k_{\text{cat}}/K_M)_{\text{Im}}^{\text{ATP}} = 8 \text{ M}^{-1} \text{ s}^{-1}$ for the reaction of H122A·Im with ATP.³ The velocity equation shown below the model in Scheme 3 is a simplified version of the general velocity equation for this model that holds when ATP is subsaturating, as was the case for all experiments reported herein.

² A random binding model is presented, although the data do not allow it to be distinguished from an ordered binding model for ATP and Im. One might expect that the H122A reaction follows an ordered mechanism, with Im binding first and ATP binding second, because Im may not be able to access the nucleophile cavity after ATP binds. However, transfer of the phosphoryl group is slow relative to binding steps, so that all of the enzyme·substrate complexes depicted reach equilibrium prior to reaction; the kinetic measurements therefore do not distinguish between these binding models. The ordered binding model is a special case of the random binding model that is presented. The conclusions drawn herein hold whether or not binding is ordered.

³ A caveat to this analysis is that the Im concentration range for measurements could not be extended much beyond the apparent K_d . It is therefore possible that the downward curvature observed for the Im dependence of the H122A reaction with ATP (Figure 7) represents experimental error. If this were the case, the $(k_{\text{cat}}/K_M)_{\text{Im}}^{\text{ATP}}$ value reported for H122A would be a lower limit. However, the third-order rate constant (k_3) for the reaction of enzyme, ATP, and Im is independent of this caveat, because it represents reaction at subsaturating Im concentrations. Comparison of this rate constant for H122A and H122G reveals that k_3 for H122G is 10^4 -fold greater than the k_3 for H122A. Thus, the caveat described above does not affect the conclusion that the reaction of Im in the H122A active site is severely hindered relative to the reaction of Im in the H122G active site.

Crystallization and Structure Solution of H122A NDPK. Crystallization occurred in a few days in hanging drops containing 10% PEG 600, 20 mM MgCl_2 , 50 mM Tris-HCl, pH 7.5, and 12.5 mg/mL H122A over wells containing 20% PEG 600 in the same buffer. The crystals belong to hexagonal space group $P6_322$ with cell parameters $a = b = 75.0 \text{ \AA}$ and $c = 106.2 \text{ \AA}$ and have a monomer in their asymmetric unit.

X-ray diffraction data were collected on a rotating anode (Rigaku), using a single crystal that was flash-cooled in liquid nitrogen and kept at 100 K during data collection using an Oxford Cryosystem. The station was equipped with a RAXIS-IIc image plate. Data processing was performed with DENZO (14) and data reduction with ScalePack. Further processing used the CCP4 program suite (15). Statistics are reported in Table 1.

The space group of the H122A crystals was the same as for wild-type *Dictyostelium* NDPK (16). Thus, the orientation of the molecule was checked by molecular replacement using this complex as a search model. An electron density map clearly showed the replacement of the His 122 side chain by an Ala side chain. The structure was refined using CNS (17). The final model has an R factor of 16.6% at 1.9 \AA resolution (Table 1).

Calculation of Molecular Volumes. Molecular volumes were calculated by first building and energy-minimizing the molecules, using the program Chem 3D Pro 5.0 (Cambridge-Soft). The coordinates obtained were used in the programs of Connolly (18) with a probe radius of 1.4 \AA . The atomic radii used were as follows: C, 1.7 \AA ; H, 1.2 \AA ; N, 1.5 \AA ; O, 1.4 \AA ; aromatic C, 1.3 \AA .

RESULTS

The cavity created by mutation of histidine 122 to glycine in NDPK is accessible to solvent and bordered by the charged residue glutamate 133. These properties of the H122G cavity distinguish it from the largely hydrophobic cavities that have been systematically rescued by small molecules in previous studies (e.g., refs 7–10). To probe molecular properties of this hydrophilic cavity, the ability of alcohols to rescue phosphoryl transfer was examined. Rescue by the alcohols was then correlated with physical characteristics of the alcohols. Rescue is a stringent criterion because it requires that the alcohol not only enter the cavity but also become appropriately oriented and then react with ATP.

Reactions of Alcohols with ATP and H122G. Addition of alcohols to reaction mixtures containing $\text{Mg}\cdot\text{ATP}$ and H122G typically resulted in production of the corresponding alkyl phosphate products. Ion-exchange HPLC was used to separate alkyl phosphate and P_i products generated from competing nucleophilic attack on ATP by alcohols and water, respectively, so that partitioning between reaction with the alcohol and reaction with water could be followed. The fraction of alkyl phosphate product was proportional to the molar fraction of alcohol in the reaction, indicating that alkyl phosphate formation involved only a single alcohol in all cases. This constancy also indicates that there are no significant effects on the relative reactivity from changing the solvent composition. Because the alcohol and water compete for reaction, the relative product formation is described by the ratio of rate constants shown in Scheme 1

(19). Thus, the rate constant for reaction of the alcohol relative to that for reaction of water, k_{rel} , could be calculated from the fraction alkyl phosphate formed and the molar concentrations of nucleophilic alcohol ($[\text{ROH}]$) and water present, according to the equation in Scheme 1. These relative rate constants are shown in Table 2.

As mentioned above and in the Experimental Procedures, the amount of alkyl phosphate product was proportional to the concentration of alcohol present in all cases. Thus, the alcohol is subsaturating. It should be emphasized that although there are numerous potential binding modes for the alcohols within the active site cavity, only the subset of binding modes that allow reaction are probed in the experiments herein, because the reaction measured is as follows: $\text{E} + \text{ROH} + \text{ATP} \rightarrow [\text{E} \cdot \text{ATP} \cdot \text{ROH}]^\ddagger$.⁴ This is exactly analogous to the situation with nonproductive binding, which can decrease k_{cat} and K_{M} , but has no effect under subsaturating conditions, i.e., no effect on $k_{\text{cat}}/K_{\text{M}}$ (19).

Below we correlate the measured reactivity of each alcohol with properties of the alcohol in order to identify properties that affect rescue in the H122G cavity.

Effect of Solution Reactivity and pK_{a} on Alcohol Reactivity. The reactions of ATP with a subset of the alcohols in Table 2 have previously been studied nonenzymatically (20). The simplest model predicts that the alcohols would react similarly with ATP, relative to water, within the H122G cavity and in solution. We considered this model by plotting the enzymatic and nonenzymatic data together in Figure 2A, in which the reactivity of each alcohol within the H122G cavity is plotted as a function of its reactivity in solution. If the data fell on a straight line with a slope of one (Figure 2A, dashed line; note the different scales on the axes), this would suggest that a given alcohol reacts analogously within the H122G cavity and in solution. However, the data appear to be uncorrelated, indicating that the reactivities of alcohols within the H122G cavity are altered with respect to their reactivities in solution. Two additional observations can be made from Figure 2A. First, the enzymatic rate constants encompass a much greater range of values than the solution rate constants. Second, the reaction of water is more favorable than reactions of alcohols in the cavity, despite their similar solution reactivities.

An alternative way to compare the reactivities of alcohols in solution to their enzymatic reactivities is to consider the respective nonenzymatic and enzymatic Brønsted relationships. A Brønsted relationship correlates the pK_{a} values (proportional to the standard free energy change of protonation) of a series of nucleophiles with $\log k$ (a linear function of the free energy of activation, where k is the rate constant for nucleophilic reaction). These data typically fall on a straight line for reactions in solution, as the ability of a nucleophile to donate electrons in a bond to a proton (pK_{a}) tends to be closely related to its ability to donate electrons to form a partial bond to an electrophile in a transition state ($\log k$). The slopes of such linear free-energy relationships are referred to as $\beta_{\text{nucleophile}}$ values, and they provide measures

⁴ As represented in the reaction in the text, ATP is also subsaturating in these experiments. Nevertheless the same relative reactivities for subsaturating alcohols would hold with saturating ATP ($\text{E} \cdot \text{ATP} + \text{ROH} \rightarrow [\text{E} \cdot \text{ATP} \cdot \text{ROH}]^\ddagger$), as the reaction step: $\text{E} + \text{ATP} + \text{ROH} \rightarrow \text{E} \cdot \text{ATP} + \text{ROH}$ is independent of the alcohol (see also footnote 2).

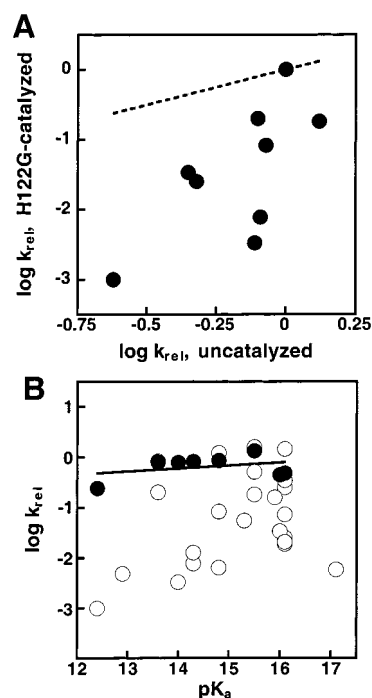


FIGURE 2: Dependence of H122G-catalyzed phosphoryl transfer from ATP on the nonenzymatic reactivity (A) or pK_{a} (B) of the alcohol nucleophile. Enzymatic data are from Table 2, and nonenzymatic data are from ref 20. The dashed line in panel A represents a model in which the alcohols react similarly with ATP, relative to water, within the H122G cavity and in solution; the line has a slope of one and includes the point corresponding to the reaction of water. The solid line in panel B is a least-squares fit to the nonenzymatic data (●) and gives a slope of $\beta_{\text{nucleophile}} = 0.07$, whereas the enzymatic data (○) appear to be uncorrelated.

of the bonding present in the transition states of reactions (21–23). The Brønsted relationship for reactions of alcohols with ATP in solution is well described by $\beta_{\text{nucleophile}} = 0.07$ (Figure 2B; closed symbols) (20). In contrast, the enzymatic reactivity data from Table 2 does not follow this linear relationship (Figure 2B; open symbols). Further, there is much more scatter in the enzymatic reactivity data. Thus, the reactivities of individual alcohols are influenced by the H122G cavity, and these energetic side effects obscure any information about the transition state that may otherwise be gleaned from this approach.

Effect of Size on Alcohol Reactivity. One anticipated effect of requiring alcohols to react with ATP from within a restricted cavity is steric exclusion of alcohols that do not fit inside the cavity. The simplest model predicts that the alcohols would react similarly to water, as they do in solution (20), up to a certain size cutoff, whereupon they would be excluded from the cavity. This model is depicted as a dashed line in Figure 3, where the expected size cutoff has been approximated by the molecular volume of 4-methylimidazole, which represents the deletion from wild-type NDPK in the H122G mutant.

We tested this model by considering the reactivity of the unsubstituted primary alcohols from Table 2. The alcohol reactivities are plotted in Figure 3 in order of increasing molecular volume. Their behavior is more complicated than expected from the simple exclusion model described above. Methanol, ethanol, and propanol react 6–40-fold more slowly than water, despite their similar reactivities in solution and their small size relative to the size of the cavity. The

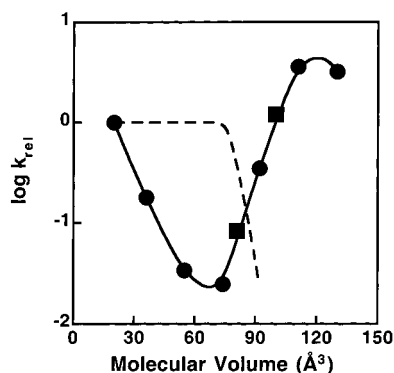


FIGURE 3: Dependence of H122G-catalyzed phosphoryl transfer from ATP on the molecular volume of unsubstituted primary alcohols (●). Methoxyethanol and ethoxyethanol are included for comparison (■). The dashed line represents the behavior expected from a simple size exclusion model, in which the alcohols react similarly until they approach the molecular volume of 4-methylimidazole, whereupon they are excluded from the cavity. The solid line is drawn through the data solely to guide the eye and does not represent a particular model. The data are from Table 2. The following molecular volumes were calculated as described in the Experimental Procedures: water, 20 Å³; methanol, 36 Å³; ethanol, 55 Å³; propanol, 74 Å³; methoxyethanol, 81 Å³; butanol, 92 Å³; ethoxyethanol, 100 Å³; pentanol, 110 Å³; hexanol, 130 Å³; 4-methylimidazole, 76 Å³.

reactivity of butanol approaches the reactivity of water, while the reactivities of pentanol and hexanol exceed the reactivity of water. The observation described below, that the presence of Ala at position 122 instead of Gly inhibits reaction with these alcohols, suggests that the alcohols are situated, at least in part, within the H122G cavity during reaction. Further, there is no indication from the structure of substantial flexibility surrounding the cavity for the H122G mutant that might allow reactivity from an altered active site configuration (11), and the crystallographic temperature factors (*B* values) for residues in the cavity are similar for the H122G and H122A mutants (data not shown).

A reasonable explanation for the reactivity results is that the smaller alcohols react poorly because they disrupt solvation by water inside the cavity. According to this model, larger alcohols may better occupy the cavity by replacing water molecules that make suboptimal interactions within the cavity with the added methylene groups, resulting in faster reaction rates. The observation that pentanol and hexanol, alcohols with molecular volumes that clearly surpass the molecular volume of the cavity, react even more favorably than water suggests that these alcohols additionally make favorable interactions with the protein outside of the cavity. Consideration of the H122G structure reveals a cleft at the base of the mutant active site cavity that may accommodate the aliphatic tail of long-chain alcohols (Figure 4). This may allow favorable interactions and reaction with ATP despite these alcohols having volumes that exceed the volume of the cavity created by the mutation.

Effect of Shape on Alcohol Reactivity. Double or triple bonds and branching affect the shape of alcohols, so we analyzed the ability of alcohols that contain these features to rescue phosphoryl transfer in the H122G cavity. Data for alcohols with double or triple bonds are combined in Table 3. Histidine, the canonical nucleophile of NDPK, is planar, and double or triple bonds induce planarity in the alcohols. The simplest model therefore predicts that unsaturated

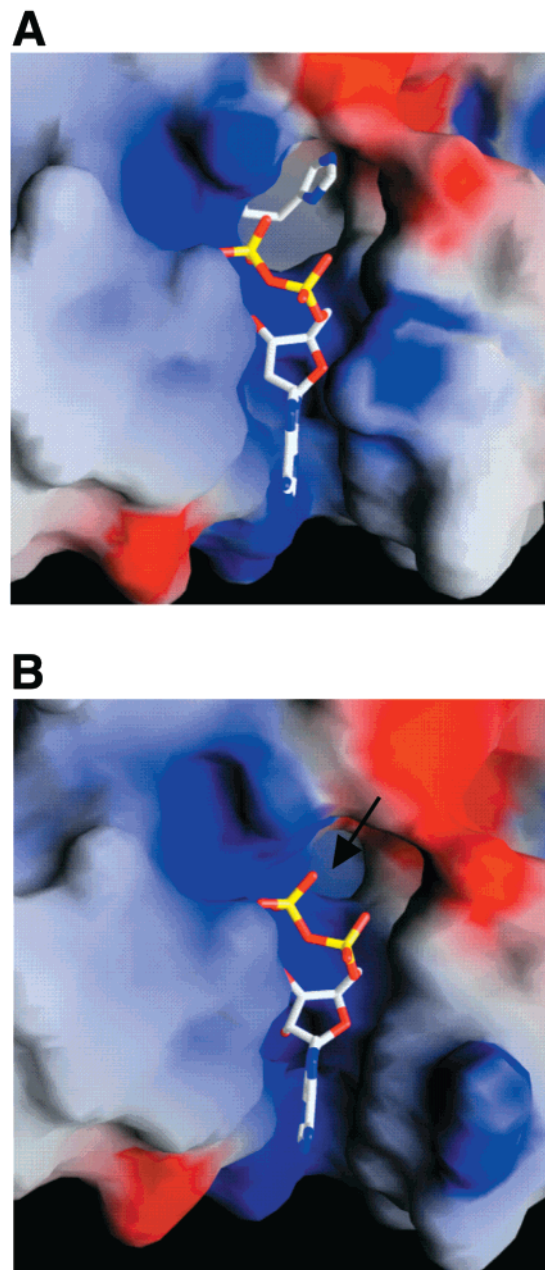
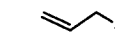
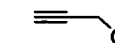
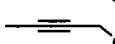
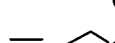



FIGURE 4: Model of the molecular surface at the active site. (A) Wild-type NDPK with bound nucleotide and the covalent His 122 nucleophile in stick representation (51). (B) H122G NDPK with bound nucleotide in stick representation (11). A cleft at the base of the nucleophile cavity (arrow, top center) may accommodate the aliphatic tail of long-chain alcohols, allowing them to react with ATP despite having volumes that exceed the volume of the cavity created by the mutation. This cleft is blocked by His 122 in the wild-type structure. Created with GRASP (52).

alcohols would be more reactive than the corresponding saturated alcohols because their shape mimics the shape of the canonical nucleophile. Alcohols containing double or triple bonds between carbons 2 and 3 (compounds 1–3) do indeed react faster than the corresponding saturated alcohols. In contrast, alcohols that are unsaturated between carbons 3 and 4 (4, 5) react more slowly than their parent alcohols (Table 3, sat. ROH). These results are consistent with the simple model described above. Alcohols that are unsaturated at proximal positions are planar and compact, like histidine, so they react faster than their parent alcohols. Alcohols that are unsaturated at distal positions are planar and extended,

Table 3: Alcohol Reactivity as a Function of Bond Order^a

Unsaturated ROH	Number of carbons	Position of unsaturation	k_{rel} (unsat. ROH) ^b	k_{rel} (sat. ROH) ^c	Ratio of k_{rel} values ^d
 (1)	3	2,3	0.51	0.025	20
 (2)	3	2,3	0.20	0.025	8
 (3)	4	2,3	0.83	0.35	2
 (4)	4	3,4	0.055	0.35	0.2
 (5)	4	3,4	0.16	0.35	0.5

^a 25 °C, 50 mM potassium EPPS, pH 7.8, 5 mM MgCl₂, *I* = 0.3 M (KCl). Values of k_{rel} are from Table 2. ^b k_{rel} for the pictured unsaturated ROH. ^c k_{rel} for the saturated ROH with the same number of carbons as the pictured unsaturated ROH. ^d Ratio = k_{rel} (unsat. ROH)/ k_{rel} (sat. ROH)

unlike histidine, and are not favored over their parent alcohols; the decreased reactivity may be due to the restricted ability of these alcohols to rearrange and minimize unfavorable interactions or to make favorable interactions.

Branched alcohols that were investigated all react more slowly than unbranched alcohols with the same number of carbons (Table 2). The deleterious effects of branching range from 5- to 100-fold, depending on the number of carbons and the position of the branch within the alcohol. We have already noted how difficult it is for small flexible primary alcohols to be accommodated for reaction within the cavity, so it is not surprising that reactions of the bulkier and more constrained branched alcohols are even less favorable.

Effect of Polarity on Alcohol Reactivity. The H122G cavity also appears to discriminate against polar nucleophiles. For example, fluoroethanol, difluoroethanol, and trifluoroethanol have reactivities that are ~4-, 7-, and 30-fold lower than their parent alcohol, ethanol (Table 2). Nevertheless, there is one striking exception. Chloropropanol reacts ~60-fold faster than its parent alcohol, propanol, and similarly to water ($k_{rel} = 1.6$). The exceptional reactivity of chloropropanol relative to its parent alcohol and to other polar nucleophiles is presumably due to a fortuitous binding site for the terminal chloromethyl group within the H122G cavity.

Differential Effect of Substituents on the Reactivity of Amines and Alcohols. Previous studies demonstrated that small amine nucleophiles react with ATP within the H122G cavity mutant (11). The simplest model predicts that amines and alcohols with the same R group would rescue phosphoryl transfer analogously. This is because an R group would be expected to pack similarly in the H122G environment whether attached to an amine or an alcohol, as the -OH and -NH₂ groups are similarly constrained within the active site due to their partial bond to ATP in the transition state monitored in these experiments.

Amine reactivity data from the earlier work was combined with the alcohol reactivity data from Table 2 to create Figure 5, in which the reactivity of each amine is plotted as a function of the reactivity of the alcohol that possesses an identical R group. If the data fell on a straight line with a slope of one, this would indicate that a given R group affects rescue analogously in both amine and alcohol contexts (Figure 5, dashed line). However, the enzymatic data do not follow this dependence; the different R groups have a larger effect on alcohol reactivity than on amine reactivity. The data thus suggest that the R group and its packing in the cavity affect the environment about the attacking atom and

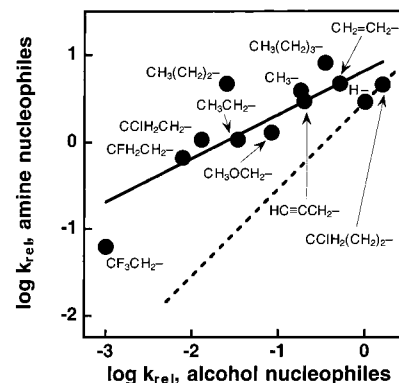


FIGURE 5: Comparison of the reactivities of alcohol (ROH) and amine nucleophiles (RNH₂) with identical R groups in H122G-catalyzed phosphoryl transfer from ATP. R groups are depicted adjacent to the relevant data. The solid line is a least-squares fit to the data with a slope of 0.50 and is drawn solely to guide the eye. The dashed line has a slope of one and includes the point representing the parent compounds (R = H), water and ammonia. Alcohol data are from Table 2, and amine data are from ref 11.

that there is a differential effect for -OH and -NH₂. Solvation effects within the cavity could be responsible for these results, as alcohols and amines have different numbers of hydrogen bond donors and acceptors and form hydrogen bonds of different strengths (24).

Solvation within a Restricted Cavity Appears to be an Important Determinant of Reactivity. Models based upon nonenzymatic reactivity, steric exclusion, shape, polarity, or analogous effects of identical R groups cannot simply account for the rescue results. The reactivity analysis reveals that the reaction of water is more favorable than reactions of alcohols in the cavity, despite the similar reactivities of water and alcohols in solution and the ability of the alcohols to fit into the cavity. This lower reactivity of alcohols suggests that the alcohols disrupt solvation and that their interactions with the cavity are unable to compensate for the loss of interactions of the attacking water molecule with other water molecules within the cavity. Furthermore, the absence of a direct correlation between the reactivities of amines and alcohols with identical R groups may reflect the difficulty of meeting the different solvation requirements for amines and alcohols within this restricted cavity.

The importance of solvation is likely to be related to the limited extent to which this cavity is accessible to solvent and to the proximity of the cavity to the carboxylate of glutamate 133, which is expected to interact strongly with water. Consider an alcohol that readily fits within the cavity.

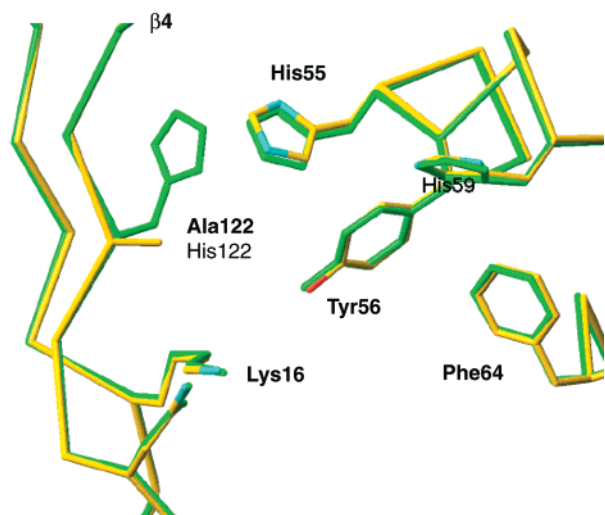


FIGURE 6: Superposition of the H122A structure (colored by atom type) with wild-type NDPK (in green) (16). Both structures were solved in the absence of nucleotide. In the H122A structure the presence of the Ala 122 methyl group, only 2.4 Å from the imidazole ring of the His 122 (wild-type), may account for the poor reactivity of Im in the H122A active site. In related structures of wild-type NDPK with nucleotide bound, His 59 interacts with the α -phosphate, Phe 64 interacts with the base and ribose, Lys 16 interacts with the ribose and the γ -phosphate, and Tyr 56 interacts with the γ -phosphate (51, 53, 54). C_{α} atoms of the respective structures were used to produce this superposition.

The ground state for the alcohol reaction has water in the cavity and alcohol solvated in solution. The low reactivity of the alcohol relative to water suggests that there is an energetic penalty for positioning of the alcohol in the active site in its transition state configuration, and the variable reactivity of the alcohols suggests that this penalty is highly dependent upon the R group. It is presumably difficult to accommodate alcohols in the cavity with optimal steric and electrostatic features. Even if water molecules are present to allow improved steric packing and van der Waals interactions, it is unlikely that these water molecules can make the same number of hydrogen bonds or have the same freedom of motion as in the cavity occupied by a reacting water molecule surrounded by other water molecules.

Comparison of Nucleophile Reactivities within the H122A and H122G Cavity Mutants. If properties of the cavity have profound effects upon rescue, as the reactivity results described above suggest, then changing the cavity should change the rescue profile. We turned to H122A, a second nucleophile cavity mutant of NDPK, to investigate this possibility. H122A differs from H122G only by the presence of an additional methyl group in the cavity. Because these mutant proteins are structurally similar (see below) and possess nucleophile cavities of similar sizes, they are a useful pair for investigating the energetic effects of choosing different deletion mutants in site-directed mutagenesis.

Structural studies of the two mutants reveal that the proteins are essentially superimposable with their wild-type counterparts. Previous work revealed that the structure of H122G with nucleotide bound is superimposable with the structure of wild-type NDPK with nucleotide bound, resulting in a root-mean-square distance between equivalent C_{α} atoms of 0.38 Å (11). The H122A structure was solved in the absence of nucleotide and can be compared with the structure of unliganded wild-type NDPK (Figure 6) (16). The mutant

Table 4: Rate Constants for Reactions of H122G and H122A^a

nucleophile	H122G	H122A	ratio
A.	$(k_{\text{cat}}/K_M)^{\text{ATP}} (\text{M}^{-1} \text{s}^{-1})^b$		
H ₂ O	1000 ^c	600	2
Im	40 000 ^c	8	5000
B.	k_{rel}^d		
CH ₃ OH	0.18	0.006	30
CH ₃ CH ₂ OH	0.034	<0.001	>34
CH ₃ (CH ₂) ₂ OH	0.025	<0.001	>25
CH ₃ (CH ₂) ₃ OH	0.35	<0.001	>350
CH ₃ (CH ₂) ₄ OH	3.6	<0.009	>400
CH ₃ (CH ₂) ₅ OH	3.2	<0.05	>64

^a 25 °C, 50 mM potassium EPPS, pH 7.8, 5 mM MgCl₂, $I = 0.3 \text{ M}$ (KCl). ^b The second-order rate constants are defined in Scheme 2. ^c From ref 11. ^d k_{rel} is defined in Scheme 1. ^e Data are from Table 2.

protein has the same quaternary (hexameric) and tertiary structure as the wild-type protein. Overall, the root-mean-square distance between equivalent C_{α} atoms in the two structures is 0.19 Å. Locally, the mutation has little effect, as the C_{α} position of residue 122 moves by less than 0.8 Å and the main-chain conformations of the respective β 4 strands are similar (Figure 6). As reported for the H122G structure, the Glu 133 side chain whose carboxylate accepts a hydrogen bond from His 122 in the wild-type protein, helping to orient its imidazole group, retains its position and conformation in the H122A mutant. Because the H122A and H122G mutant structures have been solved in different nucleotide contexts, they are not themselves directly superimposable. Nevertheless, the structural similarities between these proteins and their respective wild-type counterparts suggest that replacement of His 122 by either Gly or Ala has little effect on the three-dimensional structure, even locally.

We initially examined the reaction of ATP and water in the H122A cavity. The ATP hydrolysis reaction catalyzed by H122A proceeds with a $(k_{\text{cat}}/K_M)_{\text{H}_2\text{O}}^{\text{ATP}}$ value of 600 $\text{M}^{-1} \text{s}^{-1}$ (Scheme 2), within 2-fold of the corresponding rate constant for the H122G reaction (Table 4A). This result suggests that water behaves similarly in the respective cavities, despite the presence of an additional methyl group in the H122A cavity.

Quite different results were obtained, however, when the reactions of the mutant enzymes with Im as a nucleophile were compared. Addition of Im to reaction mixtures containing ATP and H122A resulted in formation of an ImP product, but preliminary observations suggested that the amount of ImP formed was dramatically less than it had been for identical reactions containing H122G (11). To quantitate this difference $(k_{\text{cat}}/K_M)_{\text{H}_2\text{O}}^{\text{ATP}}$ for H122A was measured, which required that the enzyme be saturated by Im (Scheme 2). However, at the highest Im concentrations, a modest downward curvature was observed in the Im dependence of the H122A reaction with ATP (Figure 7), as had been seen previously in the Im dependence of the H122G reaction with ATP (11). As in the earlier work, this curvature was presumed to arise from binding of an inhibitory Im, in addition to the Im that binds and rescues in the nucleophile site (Scheme 3). Data were treated as described in the Experimental Procedures and give $(k_{\text{cat}}/K_M)_{\text{Im}}^{\text{ATP}} = 8 \text{ M}^{-1} \text{s}^{-1}$ for the reaction of H122A·Im with ATP (Figure 7; Table 4A).³ This rate constant is 5000-fold less than the value of

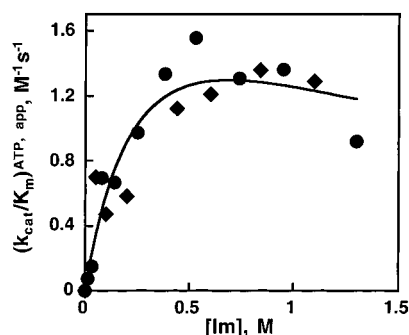
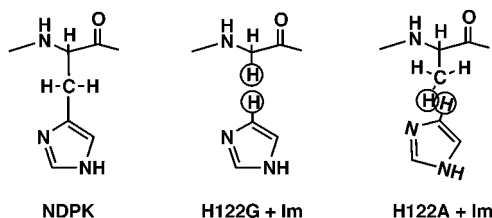


FIGURE 7: Im binding and saturation for H122A NDPK. Different symbols represent data from independent experiments. Data are fit to the two Im model shown in Scheme 3, with K_i for the inhibitory Im set to 0.45 M as described in the Experimental Procedures; $K_d = 1.0$ M for the functional Im and $(k_{cat}/K_M)^{ATP}_{Im} = 8 \text{ M}^{-1} \text{ s}^{-1}$ are obtained.³ The data in the plot does not reach this $(k_{cat}/K_M)^{ATP}_{Im}$ plateau because the rate increase corresponding to saturation of the nucleophilic Im is masked by inhibition from the second site Im, which also results in the downward curvature at high Im concentrations.

Scheme 4



$(k_{cat}/K_M)^{ATP}_{Im}$ measured for reaction of H122G·Im with ATP (Table 4A). Modeling of Im within the H122A cavity suggests a straightforward reason for the low reactivity of Im: steric clash prevents the methyl group of H122A and Im from simultaneously occupying the cavity, as represented in Scheme 4.

Similar results have been obtained in related systems. Hexose-1-phosphate uridylyltransferase catalyzes the interconversion of UDP-galactose and glucose-1-phosphate to UDP-glucose and galactose-1-phosphate via a covalent histidine intermediate. Frey and co-workers replaced the histidine nucleophile with glycine (H166G) or alanine (H166A) in this transferase, and Im rescued the mutant enzymes for reaction with UDP-glucose (25–27). Comparison of the rate constant $(k_{cat}/K_M)^{UDP-glucose}$ for Im-rescued H166G and Im-rescued H166A transferases [analogous to $(k_{cat}/K_M)^{ATP}_{Im}$ for H122G·Im and H122A·Im; Scheme 2] revealed a 1200-fold advantage for the H166G variant, similar to the 5000-fold advantage for Im-rescued H122G NDPK relative to Im-rescued H122A NDPK (Table 4A). These authors also concluded that additional steric bulk in the vicinity of the β -carbon of the nucleophilic histidine hindered rescue of the alanine mutant (27). Likewise, chemical rescue of glycine mutants but not of the corresponding alanine mutants has been observed for replacement of a histidine in myoglobin (28, 29) and a lysine in rhodopsin (30).

The reactivity results for Im and water as nucleophiles in the H122G and H122A reactions represent two extremes. The two enzymes catalyze the reaction of water and ATP by essentially the same amount, but H122G is a much better catalyst of the reaction of Im and ATP than is H122A,

presumably because Im is sterically excluded from the H122A cavity. We expanded the reactivity comparison to include nucleophiles that are intermediate in size between water and Im by investigating the ability of H122A to catalyze phosphoryl transfer from ATP to a series of alcohols, using the same approach described above for H122G (Scheme 1).

The data for reactions of alcohols with ATP in the H122A active site are summarized in Table 4B. Surprisingly, considering that the reactivity of water is similar in the two mutant contexts (Table 4A), the k_{rel} for methanol is 30-fold smaller in the H122A context than in the H122G context. Only limits could be obtained for the reactions of larger alcohols in the H122A context, even though their reactions were readily detected in the H122G context (Table 4B). There is no simple structural basis for discrimination against the smaller alcohols by H122A, as the H122A cavity is large enough to accommodate alcohols smaller than pentanol. (Pentanol and hexanol may be sterically excluded from the H122A cavity, as described above for Im.)

The cavities of H122A and H122G differ by only a single methyl group, yet the rescue profiles of the two mutants differ greatly. This observation supports the conclusion that properties of the cavity, beyond simple steric constraints, have substantial effects upon rescue. As described below, the different rescue profiles for the two mutants also warn that interpretation of the results of site-directed mutagenesis is not as straightforward as it is sometimes presented.

DISCUSSION

Implications for the Evolution of an Alcohol Kinase. Lacking the histidine nucleophile of wild-type NDPK, H122G is able to catalyze the phosphorylation of a variety of small molecules by ATP. Thus, the H122G cavity mutant can be considered a model for a primitive kinase. Unexpectedly, this kinase exhibits moderate specificity for particular alcohol nucleophiles. For example, H122G can discriminate between alcohols as similar as chloroethanol and chloropropanol by 3 kcal/mol (Table 2). As described above, steric effects, solvation within the cavity, van der Waals packing, and fortuitous interactions with certain alcohols appear to confer specificity upon this kinase. Indeed, a single methyl group influences specificity, as H122G and H122A have the same reactivity with water, but only H122G exhibits robust reactivity with a number of the alcohols tested (Table 4B). Although phosphorylation specificity appears to arise readily from properties of the cavity and the surrounding protein environment, H122G is limited by its failure to simultaneously eliminate the competing reaction of water with ATP. This engineered kinase illustrates the challenge that a primitive enzyme must overcome as it evolves to favor substrates other than solvent.

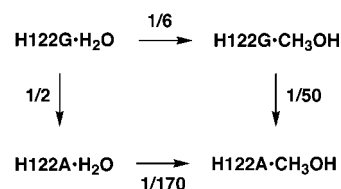
Implications for Enzymatic Linear Free-Energy Relationships. It has previously been noted that properties of enzyme active sites are likely to influence the reactivity of individual nucleophiles, complicating interpretation of enzymatic Brønsted relationships (11, 31, 32). This limitation is exemplified by the H122G results depicted in Figure 2B. The absence of anticipated steric clash is not sufficient to justify the interpretation of linear free-energy relationships in enzyme active sites, as properties including solvation, shape, and

polarity may also have profound effects on reactivity. These results underscore the need to exercise caution when applying physical organic chemistry to the study of enzymes. From a practical standpoint, it is necessary to investigate a large number of reactants that vary widely in their properties to determine whether site effects distort apparent Brønsted relationships.

Implications for Site-Directed Mutagenesis. To determine the importance of a molecular interaction within a protein, an amino acid that participates in the interaction is typically replaced by an amino acid that cannot recapitulate the interaction. Replacement of one amino acid by another with a smaller side chain, such as removal of the amine moiety of lysine by mutagenesis to alanine, is generally viewed as a conservative change for such studies. A relevant thermodynamic or kinetic parameter is then measured for both the original protein and the mutant, these measurements are converted to free energies (ΔG), and the difference in free energies between the two proteins ($\Delta\Delta G$) is interpreted to be the energetic contribution of the interaction of interest (e.g., refs 33 and 34). A $\Delta\Delta G$ value obtained from such a comparison, however, includes not only the effects from removal of the specific interaction, but also unavoidable and variable effects that are determined by the nature of the surrounding protein environment and rearrangements of that protein environment, including creation of a cavity or inclusion of solvent molecules (35, 36). These effects sometimes result in free-energy changes from double mutations that do not match the sum of the free-energy changes from the individual single mutations. Context-dependent explanations are then sought for this nonadditive behavior (see, for example, refs 37–43). However, even if the free energies from double mutant cycles are additive, the protein context still exerts a profound influence on the observed energetic effects. A simple example is the common observation of large energetic consequences from mutations within a protein's core versus small effects from identical mutations at the protein's surface.

In the present study, the conclusion that energetic effects are determined by context is most vividly illustrated by comparing the results of the H122G and H122A mutations. Comparison of the reactivities of these site-directed mutants with water can be combined with the results of the chemical "mutation" of the nucleophile from water to methanol in both mutant contexts to construct the thermodynamic box in Scheme 5 (data from Table 4). Note that water and methanol have identical reactivities in solution and are both sterically accommodated within either cavity. The vertical arrows in Scheme 5 show that changing glycine 122 to alanine decreases the rate of the water reaction by 2-fold but decreases the rate of the methanol reaction by 50-fold. The

Scheme 5



horizontal arrows show that changing the nucleophile from water to methanol in the H122G context results in a 6-fold decrease in rate, while the identical change in the H122A context results in a 170-fold decrease in rate.

These results warn of the complexities of site-directed mutagenesis and, more generally, the complexities of the energetics of enzyme-catalyzed reactions. First, the deletion mutant itself can change the energetic consequences, as illustrated by Scheme 5 and by the additional examples of large differences in reactivities of identical alcohols within the nucleophile cavities of H122G and H122A found in Table 4B. More fundamentally, deleting a side chain in order to measure an absolute energetic contribution from that side chain is problematic. This is because the energetic effect from "removal" of an interaction inherently depends on what the interacting group is changed to and on the surroundings (i.e., the context).⁵ Recent related work has demonstrated the importance of context to β -sheet propensity (44–46) and to the energetic consequences of substituting hydrophobic residues for polar residues in α -helices (47; see also ref 48). Indeed, the context and positioning created by folding endow a protein with its functional properties. Thus, context-dependent effects presumably represent a fundamental feature of protein interiors and active sites.

ACKNOWLEDGMENT

We thank Jim Havranek for assistance in determining molecular volumes of alcohols. We are grateful to members of the Herschlag laboratory for comments on the manuscript.

REFERENCES

1. Warshel, A., and Russell, S. T. (1984) *Q. Rev. Biophys.* 17, 283–422.
2. Gilson, M. K., and Honig, B. (1987) *Nature* 330, 84–86.
3. Sharp, K. A., and Honig, B. (1990) *Annu. Rev. Biophys. Chem.* 19, 301–332.
4. King, G., Lee, F. S., and Warshel, A. (1991) *J. Chem. Phys.* 95, 4366–4377.
5. Honig, B., and Nicholls, A. (1995) *Science* 268, 1144–1149.
6. Shan, S. O., and Herschlag, D. (1999) *Methods Enzymol.* 308, 246–276.
7. Toney, M. D., and Kirsch, J. F. (1989) *Science* 243, 1485–1488.
8. Eriksson, A. E., Baase, W. A., Wozniak, J. A., and Matthews, B. W. (1992) *Nature* 355, 371–373.
9. Morton, A., Baase, W. A., and Matthew, B. W. (1995) *Biochemistry* 34, 8564–8575.
10. Morton, A., and Matthews, B. W. (1995) *Biochemistry* 34, 8576–8588.
11. Admiraal, S. J., Schneider, B., Meyer, P., Janin, J., Véron, M., Deville-Bonne, D., and Herschlag, D. (1999) *Biochemistry* 38.
12. Lacombe, M. L., Wallet, V., Troll, H., and Véron, M. (1990) *J. Biol. Chem.* 265, 10012–10018.
13. Gill, S. C., and Von Hippel, P. H. (1989) *Anal. Biochem.* 182, 319–326.

⁵ Even though the same mutation often gives similar energetic effects in different active sites and protein interiors, these observations demonstrate a similarity in the behavior of these protein regions, not an ability to assign absolute or intrinsic energetic contributions to individual components of these systems. The general expectation of context-dependent energetics can be illustrated by considering the consequences of forming or eliminating electrostatic interactions. The results will depend on the presence of charged, polar, or nonpolar groups in the surroundings and on their ability to rearrange (1–6); additionally, the functional groups present in the protein are changed and the ability of the mutated group and other groups to rearrange can be affected by introduction of a mutation or variant ligand.

14. Otwinowski, Z., and Minor, W. (1997) *Methods Enzymol.* 276, 307–326.
15. CCP4. Collaborative Computational Project, No. 4. (1994) *Acta Crystallogr. Sect. A* 50, 157–163.
16. Moréra, S., LeBras, G., Lascu, I., Lacombe, M. L., Véron, M., and Janin, J. (1994) *J. Mol. Biol.* 243, 873–890.
17. Brünger, A. T., Adams, P. D., Clore, G. M., DeLano, W. L., Gros, P., Grosse-Kunstleve, R. W., Jiang, J. S., Kuszewski, J., Nilges, M., Pannu, N. S., Read, R. J., Rice, L. M., Simonson, T., and Warren, G. L. (1998) *Acta Crystallogr., Sect. D* 54, 905–921.
18. Connolly, M. L. (1985) *J. Am. Chem. Soc.* 107, 1118–1124.
19. Fersht, A. R. (1998) *Structure and Mechanism in Protein Science*, pp 114–117, W. H. Freeman, New York.
20. Admiraal, S. J., and Herschlag, D. (1995) *Chem. Biol.* 2, 729–739.
21. Jencks, W. P. (1987) *Catalysis in Chemistry and Enzymology*, Dover, New York.
22. Lowry, T. H., and Richardson, K. S. (1987) *Mechanism and Theory in Organic Chemistry*, 3rd ed., Harper and Row, New York.
23. Williams, A. (1992) *Adv. Phys. Org. Chem.* 27, 1–55.
24. Jeffrey, G. A. (1997) *An Introduction to Hydrogen Bonding*, pp 12–20, Oxford University Press, New York.
25. Kim, H., Ruzicka, F., and Frey, P. A. (1990) *Biochemistry* 29, 10590–10593.
26. Thoden, J. B., Ruzicka, F. J., Frey, P. A., Rayment, I., and Holden, H. M. (1997) *Biochemistry* 36, 1212–1222.
27. Ruzicka, F. J., Geeganage, S., and Frey, P. A. (1998) *Biochemistry* 37, 11385–11392.
28. Barrick, D. (1994) *Biochemistry* 33, 6546–6554.
29. Decatur, S. M., and Boxer, S. G. (1995) *Biochemistry* 34, 2122–2129.
30. Zhukovsky, E. A., Robinson, P. R., and Oprrian, D. D. (1991) *Science* 251, 558–560.
31. Kirsch, J. F. (1972) in *Advances in Linear Free Energy Relationships* (Chapman, N. B., and Shorter, J., Eds.) pp 369–400, Plenum, New York, .
32. Hollfelder, F., and Herschlag, D. (1995) *Biochemistry* 34, 12255–12264.
33. Fersht, A. R. (1987) *Biochemistry* 26, 8031–8037.
34. Fersht, A. R., Matouschek, A., and Serrano, L. (1992) *J. Mol. Biol.* 224, 771–782.
35. Fersht, A. R. (1988) *Biochemistry* 27, 1577–1580.
36. Matthews, B. W. (1993) *Annu. Rev. Biochem.* 62, 139–160.
37. Brown, K. A., Brick, P., and Blow, D. M. (1987) *Nature* 326, 416–418.
38. Green, S. M., and Shortle, D. (1993) *Biochemistry* 32, 10131–10139.
39. Huang, Z., Wagner, C. R., and Benkovic, S. J. (1994) *Biochemistry* 33, 11576–11585.
40. LiCata, V. J., and Ackers, G. K. (1995) *Biochemistry* 34, 3133–3139.
41. Mildvan, A. S., Weber, D. J., and Kuliopulos, A. (1992) *Arch. Biochem. Biophys.* 294, 327–340.
42. Wagner, C. R., Huang, Z., Singleton, S. F., and Benkovic, S. J. (1995) *Biochemistry* 34, 15671–15680.
43. Weber, D. J., Serpersu, E. H., Shortle, D., and Mildvan, A. S. (1990) *Biochemistry* 29, 8632–8642.
44. Minor, D. L., Jr., and Kim, P. S. (1994) *Nature* 371, 264–267.
45. Otzen, D. E., and Fersht, A. R. (1995) *Biochemistry* 34, 5718–5724.
46. Minor, D. L., Jr., and Kim, P. S. (1996) *Nature* 380, 730–734.
47. Cordes, M. H. J., and Sauer, R. T. (1999) *Protein Sci.* 8, 318–325.
48. Lee, C., and Levitt, M. (1991) *Nature* 352, 448–451.
49. Jencks, W. P., and Regenstein, J. (1976) in *Handbook of Biochemistry and Molecular Biology* (Fasman, G. D., Ed.) pp 305–351, CRC Press, Cleveland, OH.
50. International Union of Pure and Applied Chemistry. Commission on Equilibrium Data. (1979) *Ionisation Constants of Organic Acids in Aqueous Solution*, Pergamon Press, Oxford.
51. Moréra, S., Lascu, I., Dumas, C., LeBras, G., Briozzo, P., Véron, M., and Janin, J. (1994) *Biochemistry* 33, 459–467.
52. Nicholls, A., Sharp, K., and Honig, B. (1992) *Proteins* 11, 281–296.
53. Cherfils, J., Moréra, S., Lascu, I., Véron, M., and Janin, J. (1994) *Biochemistry* 33, 9062–9069.
54. Xu, Y., Moréra, S., Janin, J., and Cherfils, J. (1997) *Proc. Natl. Acad. Sci. U.S.A.* 94, 3579–3583.